View metadata, citation and similar papers at core.ac.uk
brought to you by CORE
provided by Open Research Exeter

Energy-aware Dual-path Geographic Routing to Bypass Routing Holes in Wireless Sensor Networks

Haojun Huang, Hao Yin, Geyong Min, Junbao Zhang, Yulei Wu, and Xu Zhang

Abstract—Geographic routing has been considered as an attractive approach for resource-constrained wireless sensor networks (WSNs) since it exploits local location information instead of global topology information to route data. However, this routing approach often suffers from the routing hole (i.e., an area free of nodes in the direction closer to destination) in various environments such as buildings and obstacles during data delivery, resulting in route failure. Currently, existing geographic routing protocols tend to walk along only one side of the routing holes to recover the route, thus achieving suboptimal network performance such as longer delivery delay and lower delivery ratio. Furthermore, these protocols cannot guarantee that all packets are delivered in an energy-efficient manner once encountering routing holes. In this paper, we focus on addressing these issues and propose an energy-aware dual-path geographic routing (EDGR) protocol for better route recovery from routing holes. EDGR adaptively utilizes the location information, residual energy, and the characteristics of energy consumption to make routing decisions, and dynamically exploits two node-disjoint anchor lists, passing through two sides of the routing holes, to shift routing path for load balance. Moreover, we extend EDGR into three-dimensional (3D) sensor networks to provide energy-aware routing for routing hole detour. Simulation results demonstrate that EDGR exhibits higher energy efficiency, and has moderate performance improvements on network lifetime, packet delivery ratio, and delivery delay, compared to other geographic routing protocols in WSNs over a variety of communication scenarios passing through routing holes. The proposed EDGR is much applicable to resource-constrained WSNs with routing holes.

Index Terms—Wireless sensor networks, geographic routing, energy-aware routing, anchor list, routing hole.

1 Introduction

Energy conservation and load balance are two important goals in designing routing protocols for Wireless Sensor Networks (WSNs) due to two challenges [1], [2]. First, the sensor nodes are usually powered only by batteries but expected to operate for a long period; Second, it is infeasible and costly to replace or recharge batteries once sensor nodes have been deployed. Notice that the ***routing holes***, referring to an area free of nodes closer to destination [2], [3], [4], [5], [6], [7], [11], [16], [38], are hardly avoided in WSNs in various actual geographical environments such as puddles, obstacles, and buildings, and this incurs additional energy expenditure used for data delivery. In this paper, therefore, we focus on designing energy-aware geographic routing protocols regarding how to bypass routing holes for resource-constrained WSNs, which can achieve both energy efficiency by selecting the energy-optimal forwarders and load balance by employing two node-disjoint anchor lists passing through two sides of the routing holes to shift routing path.

Geographic routing, also referred to as position-based [2], [30] or localized routing [16], [19], has been regarded as an attractive approach for resource-constrained WSNs, since it exploits local location information instead of global topology information for data delivery. It is based on the prerequisite that the nodes know their actual or virtual locations, which can be made available either through a Global Position System (GPS) receiver or through some other ways [2], [37], and exchange such information with neighbors periodically or actively. Being almost stateless and distributed, geographic routing does not require dissemination of route establishment information and maintenance of routing tables at each node, thus making it efficient, scalable and promising for WSNs. A recent detailed performance evaluation and comparison on geographic routing is given in [38].

Generally, geographic routing utilizes greedy mode to route data packets when it can find a neighbor closer to the destination than the current forwarder, and switches to bypass mode once the data packets encounter a routing hole, where there is no such a node closer to destination than the current forwarder (e.g., such an issue exists for node u towards destination v in Fig. 1). To achieve our design goal, there are at least three issues to be addressed for the current geographic routing [2], [3], [5], [7], [11], [13], [16], [28]. First, how to detect

- *H. Huang is with the School of Electronic Information, Wuhan University, Wuhan 430072, Hubei, China. E-mail: hhj0704@163.com.*
- *H. Yin is with Department of Computer Science and Technology, Tsinghua University, Beijing 100081, China. E-mail: h-yin@mail.tsinghua.edu.cn.*
- *G. Min and Y. Wu are with the College of Engineering, Mathematics and Physical Sciences, University of Exeter, Exeter EX4 4QF, U.K. E-mail: g.min@exeter. ac.uk, and Y.L.Wu@exeter.ac.uk.*
- *J. Zhang is with the Department of Computer Science and Technology, Zhongyuan University of Technology, Zhengzhou 450007, Henan, China. E-mail: junbao.zhang.uestc@gmail.com.*
- *X. Zhang is with the School of Electronic Science and Engineering, Nanjing University, Jiangsu, China. E-mail: xzhang17.cs@gmail.com.*

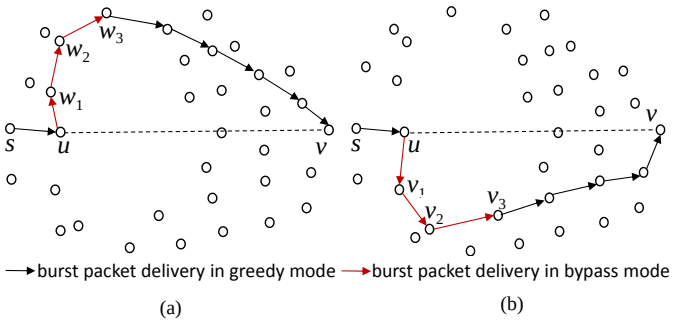

Fig. 1: Face routing bypassing the routing holes indicated by red arrows: (a) employing the right-hand rule, and (b) employing the left-hand rule.

routing holes before data delivery, since the routing holes occurring in routing will generate long path and hence consume additional resource. Second, how to bypass routing holes for load balance. Third, how to select the energy-aware forwarders and therefore guarantee that all packets are delivered in an energy-efficient manner for resource-constrained WSNs.

Currently, most geographic routing protocols, such as Greedy Perimeter Stateless Routing (GPSR) [4], Greedy-Face-Greedy (GFG) [6], and Greedy Other Adaptive Face Routing (GOAFR++) [9], tend to exploit face routing scheme to bypass routing holes, while doing not detect them before data delivery. The basic idea is to planarize the network graph using an algorithm like Relative Neighborhood Graph (RNG), or Gabriel Graph (GG) [4] and then forward messages to the destinations by employing the right-hand rule or left-hand rule [4], [6] along one or possibly a sequence of adjacent faces which all locate in the one side of the line from the source node to destination[1]. Fig. 1 elaborates an example of the face routing by employing such two rules, which detours a routing hole by forwarding the data to the node that is first traversed by the arriving edge of the packet counterclockwise or clockwise, shown in Fig. 1(a) and Fig. 1(b), respectively. There are at least two paths along the two sides of the routing hole, i.e., u-w_1-w_2-$w_3 \cdots v$ in Fig. 1(a) and u-v_1-v_2-$v_3 \cdots v$ in Fig. 1(b), provided for route recovery for data delivery. However, the right-hand rule only allows for counter-clockwise bypass traversal and the left-hand rule only allows for clockwise bypass traversal, meaning that both of them only walk along one side of the routing holes for route recovery. Beyond face routing over planar networks, there are also other bypass approaches to recover route from routing holes [7], [11], [16]. A comprehensive survey on various bypass approaches is given in [5].

These proposed protocols are simple to be implemented, whereas have a common shortcoming that they walk along only one side of the routing holes to recover the route [2], [3], [4], [5], [6], [7], [9], [10], [11], [16], [20], [28], [38]. Such approaches will make the traffic load converged on the boundary of the routing holes, and consequently achieve suboptimal network performance such as longer delivery delay and lower delivery ratio during routing packets. Furthermore, all of them cannot guarantee that all packets are delivered in an energy-efficient manner [18], [20], [24], [25], since these protocols are more inclined to route data along the boundary of the routing holes or tend to generate long path once encountering the routing holes during routing data, thereby consuming additional energy.

In this paper, we propose an energy-aware dual-path geographic routing protocol called EDGR for better route recovery from routing holes. The above-mentioned three issues are taken into account in our routing design, thus both energy conservation and load balance can be achieved. The main contributions of this paper are summarized as follows:

- EDGR establishes dual-path routing following two node-disjoint anchor lists which pass through two sides of the routing holes to route data, preventing data from being forwarded along the boundary of the routing holes. In this way, each data packet is routed to destination along two different paths in greedy mode only instead of bypass mode if possible, thereby shortening the routing length and balancing load.
- EDGR proposes a novel alternative approach to find efficient forwarder in the presence of node failure in the relay area, by introducing a random shift to the location of subdestination. Such an approach is feasible, reasonable, and energy-efficient without additional communication overhead.
- We prove that EDGR is anchor list node-disjoint and routing loop-free, and draw out its essential characteristics in terms of time complexity for anchor list building and successful routing probability.
- We extend EDGR into three-dimensional (3D) sensor networks to provide energy-aware routing for routing hole detour.
- We evaluate the performance of EDGR and its extension in a variety of communication scenarios, including varied communication sessions, network densities, and routing hole sizes. The results show that EDGR outperforms the existing energy-aware geographic routing protocols.

The remainder of this paper is organized as follows: Section 2 describes the preliminary knowledge that can benefit the understanding of the proposed EDGR scheme. The detailed EDGR is given in Section 3. Section 4 presents the theoretical analysis of EDGR. Section 5 then describes the extension of EDGR in 3D sensor networks for providing energy-aware routing. The simulation experiments and results are shown in Section 6. Section 7 provides an overview of the related work. Finally, Section 8 draws the conclusions.

1. Note that the right-hand rule and the left-hand rule are equivalent to traversing the face with the crossing edges removed. It is essential to planarize the network for face routing. If such a crossing edge exists, there must cause it failure due to routing loop.

2 PRELIMINARY KNOWLEDGE

In order to present the proposed scheme clearly, this section will introduce the preliminary knowledge including network model, energy model, lemmas and definitions.

2.1 Network Model

It is considered that no two nodes are located at the same location, as in [24], [26], [27] and so on. All sensor nodes are distributed in the network following Poisson distribution. Each sensor node knows its own location through an internal GPS device or a separate calibration process, and knows the location of neighbors and their residual energy within its maximum transmission power by exchanging beacon messages. The source node can obtain the location information of packet destinations by some destination location services [31]. The location of a node acts as its ID and its network address. Therefore, there is no need for a separate ID establishment protocol. We only consider bidirectional links, and assume that each sensor node can adjust its transmission power from 0 to its maximum transmission power. We consider the sensor nodes deployed in 2-dimensional (2D) WSNs in the first stage of our scheme design and analysis, and then extend this scheme into 3D WSNs to provide energy-efficient localized routing for routing hole detour.

2.2 Energy Model

Similar to [26] and [28], the energy consumption $c(u,v)$ used for node u sending a bit data to a neighbor v consists of four parts and can be characterized as follows:

$$c(u,v) = c_1 \cdot d(u,v)^{\alpha} + c_2 + c_3 \cdot d(u,v)^2, \qquad (1)$$

where, $d(u,v)$ denotes the Euclidian distance between nodes u and v, α is a path loss constant between 2 and 5 depending on the transmission environment, and c_1, c_2 and c_3 are some constants that are dependent on the electronic characteristics and the characteristics of the wireless devices. The parameters $c_1 \cdot d(u,v)^{\alpha}$ represents the path loss between nodes u and v, c_2 denotes the energy consumed by nodes u and v to process the signal, and $c_3 \cdot d(u,v)^2$ represents the energy used by nodes for reception in the transmission range of sender. We assume that each sensor node has the same c_1, c_2 and c_3.

2.3 Lemmas and Definitions

Let $\xi[c(u,v)]$ and N represent the energy consumption and the routing hops, respectively, for delivering one bit data from current node u to destination v. Let d_o satisfy $2c_1(1-2^{1-\alpha}) - 2c_2 + c_3 d_o^2 = 0$ and d_{opt} satisfy $c_1(\alpha-1)d_{opt}^{\alpha} - c_2 + c_3 d_{opt}^2 = 0$. The characteristics of energy consumption were investigated in [19], [26], [23], [24], [28] based on the above energy mode or its original prototype, and two lemmas were given as follows.

Lemma 1. *If $d(u,v) \leq d_o$, direct transmission is the most energy-optimal way for data delivery from node u to node v.*

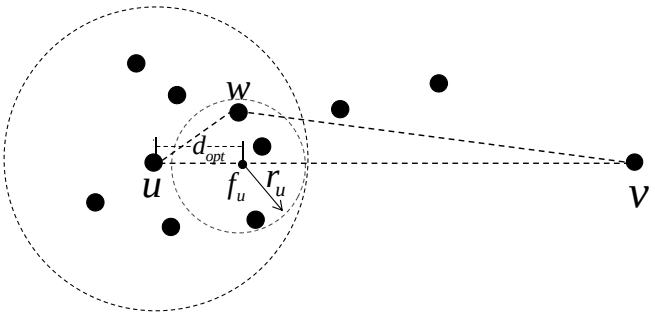

Fig. 2: Illustration of the ideal relay location and relay region for the current forwarder u.

Lemma 2. *If $d(u,v) > d_o$, $\xi[c(u,v)]$ is minimized when all hop distances are equal to $d(u,v)/d_{opt}$, and the optimal routing hops N_{opt} is $\lfloor d(u,v)/d_{opt} \rfloor$ or $\lceil d(u,v)/d_{opt} \rceil$.*

Lemmas 1 and 2 show that d_{opt} is the energy-optimal forwarding distance for minimizing $\xi[c(u,v)]$. This observation motivates us to introduce the concept of energy-optimal relay region (see Definition 2) for energy conservation.

Definition 1 (Ideal Relay Location). *The ideal relay location f_u for node u is defined as the location on the straight line from node u to the anchor node or destination v, where $d(u,f_u) = d_{opt}$.*

Definition 2 (Relay Region). *The relay region $r(u,v)$ for node u is defined as the circle area centered at f_u with radius $r(u)$, where $r(u) \leq d(u,f_u) = d_{opt}$.*

In order to make Definitions 1 and 2 clear, as shown in Fig. 2, we give an illustration of the ideal relay location, and the relay region $r(u,v)$ of node u.

3 EDGR: ENERGY-AWARE DUAL-PATH GEOGRAPHIC ROUTING

This section will present in detail the proposed EDGR protocol for bypassing routing holes in WSNs. First, the EDGR architecture is presented, and then how to obtain anchor list is introduced. Finally, we formulate how to deliver messages in an energy-efficient manner.

3.1 EDGR Architecture

The main mechanism of EDGR is to employ two node-disjoint anchor lists to guide packet delivery and select the nodes with more residual energy from energy-aware relay region as forwarders for energy conservation. Thus, the data packets are likely routed to the anchor nodes and their destinations along two paths at the energy-efficient cost.

Fig. 3 illustrates the network architecture of EDGR. The operation of EDGR is mainly divided into two phases: anchor list obtaining and data dissemination. In the first phase, the proposed EDGR scheme uses an adaptive approach to obtain two anchor lists based on the projected distance of nodes being involved in bypass mode. In the latter phase, the proposed EDGR utilizes geographic information, the residual energy and the

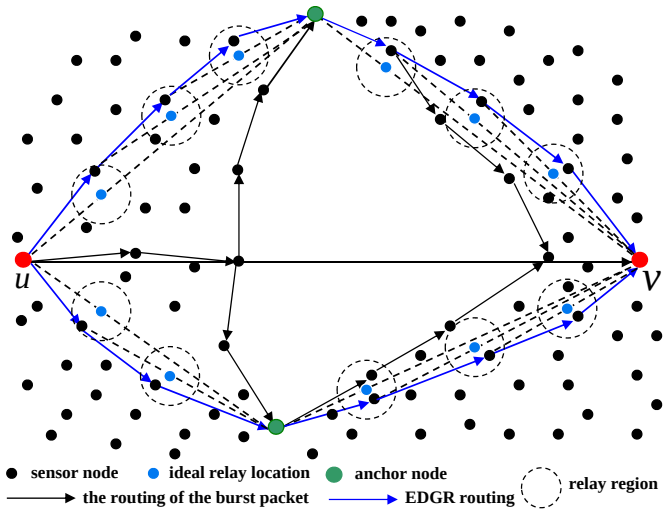

Fig. 3: The network architecture of EDGR.

characteristics of energy consumption to make routing decisions, and then unicasts the packet to the established next-hop forwarder. If there is no node in the relay region, the current forwarder then introduces a random shift to the location of the subdestination to continue data delivery.

There are three kinds of packets: beacon packet, burst packet, and data packet in our scheme. The beacon packet is used to exchange location information and residual energy among neighbors, while burst packet is used for finding the anchor lists. Fig. 4 presents the format of the burst packet. Specifically, it includes anchor lists, the locations of source node and destination. The anchor list contains a series of anchor nodes, and a flag field which indicates whether this packet bypasses the routing holes by employing the right-hand rule or left-hand rule. In addition, it includes a temporary ***void node*** in each bypass mode but is deleted finally if it violates the determined rules of anchor nodes. Here, the void node is defined as the node that switches to bypass mode from greedy mode, i.e., the node (e.g., node u in Fig. 1) which cannot find a neighbor being closer to the destination than itself, even though there is a path from the source node to destination in the network.

3.2 Anchor List Obtaining

Given source node u, it starts preparing for data dissemination by building two anchor lists.

First, it adaptively broadcasts a beacon packet to its neighbors at the maximum transmission power for announcing its location information and residual energy. Once a neighbor receives this packet, then stores such information and broadcasts a new beacon packet to its neighbors at the maximum transmission power. This process will repeat periodically among all nodes in the network, such that each node can obtain the location information and residual energy of its neighbors within their maximum transmission range.

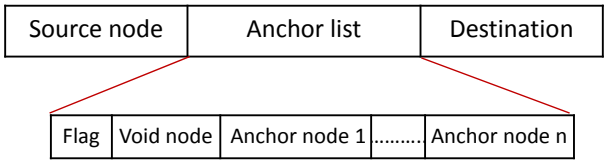

Fig. 4: Illustration of the burst packet format.

Once receiving location information and residual energy of all neighbors, source node u initiates and sends a burst packet to destination v. For any forwarder w, it uses greedy mode to forward this burst packet whenever possible and switches to bypass mode when encountering a routing hole. The bypass mode begins from the void node. For any void node w in the jth bypass mode, it first adds itself into the burst packet header (i.e., anchor list) for its downstream forwarders to decide whether to return to greedy mode. Then, it takes into consideration the following two cases to make routing decisions on how to bypass this routing hole.

Case I. If the flag is void, it copies this burst packet and then simultaneously uses right-hand rule and left-hand rule to bypass this hole, and sets the flag of two burst packets r and l, respectively, for their continued delivery relayed by the subsequent nodes in accordance with it.

Case II. If the flag is not void, this node and its subsequent relay nodes use the right-hand rule indicated by r or the left-hand rule indicated by l to detour this routing hole.

For right-hand rule or left-hand rule, let $\overrightarrow{w_{f_j} \cdots w_{l_j}}$ denote the routing of the jth bypass mode from node w_{f_j} to node w_{l_j}. Given a node w on $\overrightarrow{w_{f_j} \cdots w_{l_j}}$, we denote its projected node as w' on the line from source node u to destination v, and denote $d(w, w')$ as its projected distance, illustrated in Fig. 5. In the jth bypass mode, each node calculates the jth anchor node a_j from its upstream and downstream forwarders such that

$$\begin{aligned} a_j \equiv &\{w_i | max[d(w_{i-1}, w'_{i-1}), d(w_{i+1}, w'_{i+1})] \\ &\leq d(w_i, w'_i),\ s.t.\ w_{f_j} \leq i \leq w_{l_j}\} \cup \{w_{f_j}, w_{l_j}\} \end{aligned} \tag{2}$$

where node w_{f_j-1} and node w_{l_j-1} both work in greedy mode, and are w_{f_j}'s upstream forwarder and w_{l_j}'s downstream forwarder, respectively. For candidate node w_i, its location will be installed into the anchor list and sent to its downstream forwarder if it satisfies Eq.(2). There is no additional communication overhead for it to calculate $d(w_{i-1}, w'_{i-1})$ and $d(w_{i+1}, w'_{i+1})$ since the location information of neighbors w_{i-1} and w_{i+1} is known to it by beacon exchange.

Once the burst packet arrives at a node k such that $d(k, v) < d(w, v)$, then switches into greedy mode to continue delivery and deletes the temporary void node w (by node k) if node w violates Eq.(2). The anchor list $List(u, v)$ is obtained as the flag and the union of all a_j in all bypass modes, where all nodes are sorted in the increasing order according to their subscripts. It can be

Algorithm 1 : Building Anchor List

Require: source node u, destination v
1: $List(u,v) = [flag, \phi]$
Ensure:
2: u initializes beacon packet exchange
3: u sends a burst packet to v attached with $List(u,v)$
4: **if** $\forall w_i$ in the bypass mode receives the packet **then**
5: UPDATELIST($w_i, List(u,v)$)
6: **end if**
7: **if** u receives a feedback packet from v **then**
8: update $list(u,v) = [flag, a_1 \cdots a_j \cdots, a_m]$
9: send a burst packet to v via $a_1, a_2, \cdots, a_m$
10: **end if**
11: **if** $\forall w_i == a_k \in \{a_1, \cdots, a_m\}$ receives the packet **then**
12: send this packet to a_{k+1}
13: **else**
14: **if** $\forall w_i$ is in the bypass mode **then**
15: UPDATELIST($w_i, List(u,v)$)
16: **end if**
17: **end if**
18: **function** UPDATELIST($w_i, List(u,v)$)
19: **if** $w_i \in List(u,v)$ **then**
20: delete all nodes after w_i in $List(u,v)$
21: **end if**
22: **if** $w_i == w_{f_j}$ or $w_i == w_{l_j}$ or w_{i-1}, w_{i+1} are in bypass mode **then**
23: calculate candidate w_i according to Eq.(2)
24: add w_i to $List(u,v)$
25: send $List(u,v)$ to w_{i+1} following $flag$
26: **end if**
27: **if** $w_i == v$ **then**
28: send $List(u,v)$ to u
29: **end if**
30: **end function**

expressed as

$$List(u,v) = [flag, a_1, a_2, \cdots, a_n]. \quad (3)$$

Once destination v receives the burst packet, this means that an anchor list is built. Then, it regards the anchor nodes in $List(u,v)$ as subdestinations in the descending order according to their subscripts, and feeds it back to node u.

In order to avoid route failure in data delivery between source node and its subdestination, the last subdestination and destination, and two adjacent subdestinations, node u will send a new burst packet to the established subdestinations and then to destination v, according to the right-hand rule or the left-hand rule indicated by the flag in the anchor list, to check whether a routing hole exists. If this is true, a new anchor node determined by Eq.(2) is then installed into $List(u,v)$. The action for routing hole acknowledge from source node u to destination v going through the established subdestinations will be done even more than once, depending on the network density.

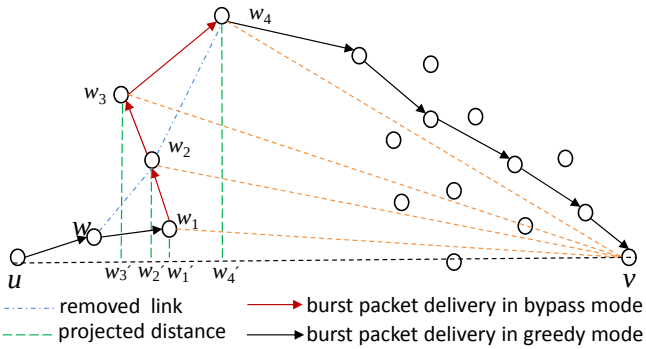

Fig. 5: Anchor list building by employing right-hand rule.

By employing right-hand rule and left-hand rule simultaneously to walk along two sides of the all routing holes, our proposed approach can obtain two node-disjoint anchor lists to guide packet delivery. With such two anchor lists, the data packets are likely routed to destinations along two different paths, thus achieving load balance.

The pseudocode of building anchor list is shown in Algorithm 1. This algorithm is initialized with the required location information and residual energy of neighbors. Then the algorithm sends a burst packet to destination v and employs both right-hand rule and left-hand rule, r and l, to bypass the all routing holes simultaneously shown in Lines 2-6 and Lines 18-30, and will update anchor list, as illustrated in Lines 7-30, if a routing hole exists between source node and its subdestination, or the last subdestination and its destination, or two adjacent subdestinations. In bypass mode, each candidate anchor node is determined by Eq.(2). Finally, two anchor lists are obtained and fed back to source node u from destination v.

Fig. 5 illustrates how to build an anchor list by employing right-hand rule, which is similar to how an another anchor list can be built if exists by employing left-hand rule. Therefore, we have only emphasized it and not depicted the nodes located below the line from source node u to destination v. The network is a partial enlarged version of the network in Fig. 1, with only one routing hole. The blue dash lines represent removed links to avoid the crossing edges existing according to the right-hand rule, nodes w_1', w_2', w_3' and w_4' are the projected nodes of nodes w_1, w_2, w_3 and w_4 on the line uv from source node u to destination v. Among all the forwarders, node w_1 is the first node, i.e., void node, which enters bypass mode to forward the burst packet due to no neighbor being closer to destination v, and node w_4 is the last node involved in such a mode to forward this packet since it can find a neighbor closer to destination v than node w_1. There are four nodes, i.e., nodes w_1, w_2, w_3 and w_4, involved in bypass mode to build an anchor list, while the other intermediate nodes only forward it. In bypass mode, nodes w_1, w_2, w_3 and w_4 first calculate their projected nodes on the line uv and projected distances, indicated by green dash lines in Fig.

5, and then calculate the candidate anchors according to Eq.(2). Finally, node w_4 is selected as the anchor node. In this way, an anchor list is obtained.

3.3 Data Dissemination

In our scheme, source node u and each forwarder regard anchor nodes as subdestinations. Before data delivery, node u randomly selects an anchor list and then embeds the anchor nodes into the data packet header.

Let $(a_1, \cdots, a_{n-1}, a_n)$ denote a sequence of anchor nodes that node u goes through towards destination v, where a_i $(1 \leq i \leq n)$ is subdestination for node u. Obviously, a_1 is its first subdestination. The following two cases are considered for making forwarding decisions.

Case I. If $d(u, a_1) \leq d_o$, based on Lemma 1, it directly sends the packet to a_1. This is because direct transmission is much more energy-efficient than relaying the packets by some intermediate nodes.

Case II. If $d(u, a_1) > d_o$, based on Lemma 2, it needs to select a forwarder for its packet delivery. Let (x_u, y_u) and (x_{f_u}, y_{f_u}) denote the coordinates of node u and its ideal relay location f_u, respectively, and let (x_{a_1}, y_{a_1}) denote the coordinates of anchor node a_1. Based on Definition 2, we have,

$$\begin{cases} x_{f_u} = x_u + \dfrac{d_{opt}}{d(u, a_1)}(x_{a_1} - x_u), \\ y_{f_u} = y_u + \dfrac{d_{opt}}{d(u, a_1)}(y_{a_1} - y_u). \end{cases} \tag{4}$$

The relay region $r(u, a_1)$ of node u is the circle area centered at f_u with radius $r(u)$ determined by the node distribution density. In such a $r(u, a_1)$, node u selects a forwarder w by employing the best combination of energy reserves and needs the minimum energy to be reached, i.e.,

$$max \quad \delta \times e_w + (1 - \delta) \times d(w, f_u). \tag{5}$$

In Eq.(5), $d(w, f_u)$ is the distance from node w to f_u, e_w is the residual energy of node w, and δ is a weight factor between 0 and 1 that determines the relative significance placed on e_w and $d(w, f_u)$. Intuitively, without considering the residual energy, some nodes may be chosen as the forwarders frequently, and thus resulting in their rapid energy depletion compared to other nodes. Therefore, EDGR is superior in energy conservation and load balance by selecting the energy-optimal forwarders. When the next forwarder w is decided, node u immediately unicasts the packet to it.

Once receiving this packet, node w first derives the location of the subdestination from the packet header, and then forwards it following the same procedure as node u. Any subdestination that receives the packet, first deletes it from the anchor list and regards the next anchor node in the anchor list as the next subdestination. This process repeats among a series of forwards and subdestinations until the packet is received by the final destination v. There may not exist any node in the current relay area. If this is the case, one natural solution is that the forwarder w increases its relay region radius to find the new neighbors. An alternative solution is that the forwarder w introduces a random shift $(\Delta x, \Delta y)$, following the 2D Gaussian distribution given by

$$f(\Delta x, \Delta y) = \frac{1}{2\pi\sigma^2} e^{-\frac{(\Delta x)^2 + (\Delta y)^2}{2\sigma^2}}, \tag{6}$$

to the coordinates (x_0, y_0) of its subdestination, in order to find the new relay region and its next-hop relay. If the packet arrives at a node in vicinity of $(x_0 + \Delta x, y_0 + \Delta y)$ but without the node within it, then the current node sends the packet to its next subdestination located behind (x_0, y_0) in the anchor list, or to the final destination v if the next anchor node is destination v.

TABLE 1: The Important Parameters and Notations

Symbol	Meaning
$\overline{d(u,w)}$	The advance that node u obtains by forwarding the packet to neighbor w
$r(u)$	The radius of $r(u, v)$
$\overrightarrow{uw_1 \cdots w_m v}$	The routing from node u to destination v
m	The number of all forwarders in bypass mode
n	The number of all routing holes
w_i'	The projected node of node w_i on $\overrightarrow{uv}$
$d(w_i, w_i')$	The projected distance between nodes w_i and w_i'
r	The communication range of nodes
R	The distance from node u to (sub)destination v
λ	The average density of nodes
$A(r, R)$	The advance area
$Prob(k)$	The probability of finding k nodes
M	$\lambda\pi r(u)^2$
N	$\lambda A(r, R)$

4 Analysis

In this section, we present extensive theoretical analysis for EDGR in terms of node-disjoint anchor list, time complexity and guaranteed delivery. In the following table, we list the important parameters and notations used in theoretical analysis.

4.1 Node-disjoint Anchor List

Property 1. *In EDGR, two anchor lists built by employing right-hand rule and left-hand rule are node-disjoint if such two anchor lists can be found.*

Proof. By simultaneously employing right-hand rule and left-hand rule to walk along two sides of the all routing holes, our proposed approach can obtain two anchor lists to guide packet delivery. In bypass mode, any selected anchor node w locates in counterclockwise side of the line from the void node to destination for right-hand rule, and clockwise for left-hand rule. This means that one anchor list decided by employing right-hand rule only contains the anchor nodes which locate in counterclockwise side of the line from the void nodes to destination, while another anchor list decided by employing left-hand rule only contains the

anchor nodes which locate in clockwise side of the line from the void nodes to destination. Clearly, such two anchor lists are node-disjoint.

Therefore, in our proposed EDGR approach two anchor lists built by employing right-hand rule and left-hand rule are node-disjoint.

4.2 Time Complexity

Theorem 1. *The time complexity for EDGR to build two anchor lists is* $\Theta(n)$.

Proof. The time complexity for EDGR to build two anchor lists is determined by the required iterative. In bypass mode, each forwarder w_i needs to calculate $d(w_{i-1}, w'_{i-1})$, $d(w_{i+1}, w'_{i+1})$ and $d(w_i, w'_i)$, then compare them to decide the anchor node according to Eq.(2), the required iterative of this step is 5. Let n_1 and n_2 denote the number of all forwarders employing right-hand rule and left-hand rule, respectively, to bypass routing holes, and let $n = n_1+n_2$. The required iterative for EDGR to build an anchor list is $\Theta(n_1)$ or $\Theta(n_2)$.

Hence, the time complexity of EDGR to build two anchor lists is $\Theta(n_1 + n_2)$=$\Theta(n)$.

The approaches, most similar to EDGR to build anchor lists, mainly include Projection Distance-based Anchor (PDA$^+$) [27] and Energy-aware Multipath Geographic Routing (EMGR) [28]. However, both of them all only build an anchor list, with the time complexity $\Theta(n_1)$ (or $\Theta(n_2)$), and $\Theta(n_1)$ (or $\Theta(n_2)$), respectively, to recover the route from routing holes. The results reveal that, similar to PDA+ and EMGR, EDGR achieves the linear time complexity to build anchor lists.

4.3 Guaranteed Delivery

Theorem 2. *EDGR is routing loop free.*

Definition 3 (Advance). *The advance* $\overline{d(u,w)}$ *that node* u *obtains by forwarding the packet to neighbor* w *towards destination* v*, is defined as the distance between node* u *and node* v *minus the distance between node* w *and node* v*, i.e.,*

$$\overline{d(u,w)} \equiv d(u,v) - d(w,v). \tag{7}$$

where $d(u,v) > d(w,v)$*. In other words,* $\overline{d(u,w)} > 0$*, meaning that each forwarder can obtain a positive advance.*

Proof. EDGR combines bypass mode and greedy mode to forward the data packets, by building the anchor list to avoid the routing holes. In this way, EDGR prevents data packet from being forwarded along the boundary of holes, thus each data packet is routed to destination node only in greedy mode instead of bypass mode if possible. So, we only need to prove its routing loop-free in greedy mode.

For any candidate node w in $r(u,v)$, shown in Fig. 2, $d_{opt} - r(u) \le d(u,v) - d(w,v) \le d_{opt} - r(u)$. Built upon Definition 2, $r(u) \le d_{opt}$. Then, we have

$$0 \le d(u,v) - d(w,v) \le min(R, 2d_{opt}). \tag{8}$$

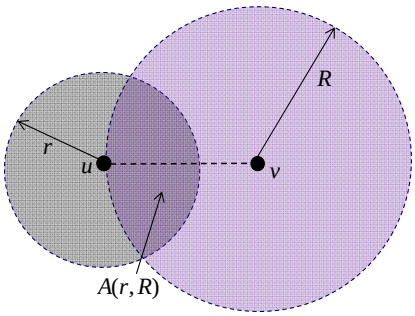

Fig. 6: The advance region for the current forwarder u to destination v.

Built upon Definition 3, $d(u,v) - d(w,v) = \overline{d(u,w)}$. This means that in our scheme each forwarder u can achieve a positive advance, although EDGR employs the combination of energy reserves and consumption to select the next hop w. Therefore, we can use the advance instead of the combination given by Eq.(5) to prove its features.

Let $\overrightarrow{uw_1w_2\cdots w_mv}$ be the routing from the source node u to destination v. Based on Definition 3, we have

$$\begin{aligned}\overline{d(u,v)} &= \overline{d(u,w_1)} + d(w_1,v) \\ &= \overline{d(u,w_1)} + \sum_{i=1}^{m-1} \overline{d(w_i,w_{i+1})} + d(w_m,v)\end{aligned} \tag{9}$$

Given any relay node $w_k (1 \le k \le p-1 \le m)$ prior to w_p in $\overrightarrow{uw_1w_2\cdots w_mv}$ between u to v, we have

$$\begin{aligned}\overline{d(w_k,v)} - \overline{d(w_p,v)} &= \sum_{i=k}^{m-1} \overline{d(w_i,w_{i+1})} + d(w_m,v) \\ &\quad - [\sum_{i=p}^{m-1} \overline{d(w_i,w_{i+1})} + d(w_m,v)] \\ &= \sum_{l=k}^{p-1} \overline{d(w_l,w_{l+1})} > 0,\end{aligned} \tag{10}$$

where $w_l (k \le l \le p-1)$ represents the relay node between nodes w_k and w_p in $\overrightarrow{uw_1w_2\cdots w_mv}$. From Eq.(10), it can be observed that the data packets are never forwarded to the previous relay nodes.

Therefore, EDGR is routing loop free.

Theorem 3. *For the current forwarder* u*, the probability that there is at least one candidate node in the relay region* $r(u,v)$ *is* $1 - e^{-\mathrm{M}}$.

Definition 4 (Advance Area). *The advance area is defined as the area of the lens formed by the intersection of two circles centered at the current node* u *and destination* v*, respectively (i.e., shaded area in Fig. 6).*

Proof. Let R denote the distance from forwarder u to anchor node or destination v, and r be the communication range of u. Given two circles with the centers separated, the advance area $A(r,R)$ from u to v can be

expressed as [36]

$$A(r,R) = r\arccos(\frac{r}{2R}) + R^2\arccos(\frac{2R^2-r^2}{2R^2}) - \frac{\sqrt{r^2(4R^2-r^2)}}{2}. \quad (11)$$

In our approach, the spatial distribution of the nodes follows 2D Poisson distribution, with the average density λ. In advance area $A(r,R)$, the probability of finding k nodes, denoted by $Prob(k)$, is

$$Prob(k) = e^{-\mathrm{N}}\frac{\mathrm{N}^k}{k!}, k \geq 0, \quad (12)$$

where N=$\lambda A(r,R)$ is the average number of neighbors in $A(r,R)$.

Based on Definition 4, it is easy to see that the advance area $A(r,R)$ of node u contains all its neighbors, which achieve the forwarding advance. Clearly, our relay region locates in $A(r,R)$. Let $\mathrm{M} = \lambda\pi r(u)^2$ be the average number of neighbors in relay region $r(u,v)$. Then, we have

$$Prob(there\ is\ a\ least\ one\ node\ in\ r(u,v)) = 1 - Prob(k=0) = 1 - e^{-\mathrm{M}}. \quad (13)$$

Hence, for each forwarder u the probability that there is at least one candidate node in the relay region $r(u,v)$ is $1-e^{-\mathrm{M}}$.

5 Extension to 3D WSNs

So far, many geographic routing protocols such as [3], [4], [6], [7], [8], [10], [11], [12], [38] and our proposed EDGR supposed that the sensor nodes are deployed in 2D sensor networks, where all sensor nodes are distributed in a 2D plane. This assumption is somewhat justified for some applications where the nodes are deployed on the earth surface and the height of the network is much smaller than transmission radius of nodes, and proven to provide drastic performance improvement over the existing sensor network routing protocols. However, such an assumption may not anymore hold true in the real-world if WSNs are deployed in complicated and challenging environments, such as atmosphere, ocean, and indoor applications. In such environments, the network nodes are distributed over a 3D space and the difference among them in the third dimension is too large to be ignored [25], [29], [30], [32], [33], [34], [35]. Recent interests in underwater sensor networks [32] and space sensor networks [33] have demonstrated great impetus to design and study 3D WSNs. In practice, 3D embedding reflects more accurate network behaviour in real-world applications. Therefore, in this section we are interested in extending our proposed EDGR routing into 3D sensor networks (called EDGR-2) to provide energy-aware routing for routing hole detour.

Similar to [25], [33] and [35], we suppose that all sensor nodes are represented by node set S in the 3D space, and have the same communication range r, which is represented as a sphere volume of radius r. Two nodes are connected by an edge if and only if the Euclidean distance between them is no more than r. Each sensor node knows: (1) the 3D coordinates (x,y,z) of its location; (2) the location and residual energy of its neighbors by beacon messages exchange periodically; and (3) the location of the destination by using a location service [31]. We consider each distance is different for every forwarder in 2D plane, regardless of greedy mode and bypass mode, to avoid degenerated cases. In fact, equal distances can be handled by using a distance function as distance measure [37].

For the forwarder u, the relay region $S(f_u,r)$ is defined as the sphere area centered on f_u with radius $r_s(u)$, where $r_s(u) \leq d(u,f_u)$. The coordinate $(x_{f_u}, y_{f_u}, z_{f_u})$ of f_u is given by

$$\begin{cases} x_{f_u} = x_u + \frac{d_{opt}}{d(u,v)}(x_v - x_u), \\ y_{f_u} = y_u + \frac{d_{opt}}{d(u,v)}(y_v - y_u), \\ z_{f_u} = z_u + \frac{d_{opt}}{d(u,v)}(z_v - z_u). \end{cases} \quad (14)$$

EDGR-2 works in two modes: greedy mode and bypass mode. In the former mode, the forwarder u selects its ideal next-hop forwarder from $S(f_u,r)$ based on the distances from the candidate neighbors to the ideal relay location f_u and its residual energy determined by Eq.(6), i.e., it sends the packet to an energy-aware neighbor that is closest to the destination than itself. If the data packets encounter a routing hole, then EDGR-2 switches into bypass mode to forward the data packets. Considering that face routing can only be used on planar topology, however there is no planar topology concept any more in 3D WSNs, EDGR-2 projects the 3D nodes into 2D plane for bypassing the routing holes. In this mode, EDGR-2 first projects 3D nodes into the xy plane, the 2D space. Then EDGR routing is performed on this projected graph. If the routing fails, i.e., a routing path cannot be found, the 3D nodes are then projected into the second plane, the yz plane. Then EDGR routing is performed again. If the routing fails again, the 3D nodes are reprojected into the third plane, the xz plane. The EDGR routing is again performed. This process continues until the data packets bypass the routing hole if possible and switches to greedy mode.

6 Performance Evaluation

In this section, we evaluate the performance of our proposed approach EDGR and its extension via simulation experiments. We first describe our simulation environments and performance metrics, and then evaluate the performance results. Finally, we show the comparison among our proposed approach, Energy-efficient Beaconless Geographic Routing (EBGR) [24], EMGR [28], and PAG-CFace(1)-PAG [25].

6.1 Simulation Setup

The popular network simulation platform, NS2.34, is used to evaluate the performance of EDGR. We select IEEE 802.11 as the MAC protocol. Unless specially noted, the number of sensor nodes randomly distributed in a 2D area of $1000m \times 1000m$ is set to 500, and varies from 400 to 600 only as the network density increases. Each source node randomly generates CBR or TCP flows at a varied speed from the range $[0.5Mbps, 1Mbps]$ with the different packet sizes, commonly set as 128 bytes, 256 bytes, or 512 bytes [2], [38]. Each sensor node has an initial energy of $1J$, and source-destination pairs are randomly selected in the network. The energy parameters are set as follows: $\alpha = 2$, $c_1 = 100pJ/bit/m^{\alpha}$, $c_2 = 100nJ/bit$, and $c_3 = 60pJ/bit/m^2$, thus the energy-optimal forwarding distance d_{opt} and d_o are $25m$ and $35.4m$, respectively, obtained from equations in Subsection 2.3. The maximum transmission range r of sensor nodes is $40m$. The IEEE 802.11 MAC protocol and wireless interface are modified to enable variable transmission ranges. It is considered that the beacon interval range of EMGR and EDGR is $[1s, 5s]$, as suggested in [8].

Each simulation experiment is run for 500 seconds, and the average performance results is collected from 40 simulation runs, which can make bypass mode more likely happen in our simulation scenarios. One or two routing holes are set in the center of the network. In each simulation scenario, the size of the routing holes can be varied to ensure that much more communication sessions can pass through them as far as possible. The communication sessions without bypass mode are not considered as our efficient results. Three basic simulation scenarios are designed to evaluate the performance of our scheme.

- **Network density scenario**: All additional nodes randomly participate in the network at the beginning of simulation experiments, and are distributed in different locations except the routing hole. The network density, denoted by ρ, referring to the mean number of neighbours per node [2], varies from the range [ρ_1 neighbors/node, ρ_2 neighbors/node]. i.e.,

$$\rho_i = \kappa_i * \frac{\pi * r^2}{1000 * 1000 - \sum_{j=1}^{k} \pi * \gamma_j^2} - 1, \qquad (15)$$

  where κ_i and γ_j denote the total number of sensor nodes and the radius of the j routing hole in the network, respectively.
- **Routing hole size scenario**: One routing hole is manually set in the center of the network. The diameter of the routing hole, defined as the longest distance between two any hole boundary nodes, varies from the range $[d_1 m, d_2 m]$ $(d_1 > 2r)$ [28]. The arbitrary two nodes are reachable to each other in the network as the routing hole size increases. By default, the fixed number of efficient communication sessions are used in the simulation experiments.
- **Communication session scenario**: All communication sessions are originated from different source nodes or delivered to various destinations. Each CBR or TCP flow ends at $490s$ to allow the emitted packets to reach their desired destinations. Two routing holes and one routing hole, with the quite large diameter, are set in 2D and 3D WSNs, respectively, to ensure much more communication sessions encounter them. The number of communication sessions, passing through the routing holes, changes from N_1 to N_2.

To have in-depth performance analysis and comparison, in addition to EDGR and its extension EDGR-2, we have also implemented the other three routing approaches: EBGR [24], EMGR [28], and PAG-CFace(1)-PAG [25] on NS 2.34. EBGR is an energy-efficient beaconless geographic routing scheme. Based on the local location and transceiver power characteristics, each node holding the data first computes its energy-aware relay region and then selects a neighbor closest to the center of the relay region as its next forwarder. EMGR is an energy-aware multipath geographic routing protocol. It utilizes the metric of advanced energy cost to select the next forwarder, and uses anchor lists passing through one side of the routing holes to shift the routing path for load balance. PAG-CFace(1)-PAG is a 3D energy-aware geographic routing based on transmission power control, which uses the low transmission range to discover neighbors and route data. Once encountering a routing hole at low transmission level, the current forwarder then increases its transmission range by a factor of β and runs neighbors discovery again. If no neighbor making progress to destination is found, it uses CFace(1) (Coordinate Face) routing to escape from the routing holes in 2D networks as soon as possible and then continues data delivery in 3D networks.

Both EBGR and EMGR are 2D energy-aware geographic routing schemes, while PAG-CFace(1)-PAG is a 3D energy-aware geographic routing approach. Therefore, in all simulation experiments, we compare the performance of EDGR with EBGR and EMGR in 2D WSNs, and then compare the performance of EDGR-2 with PAG-CFace(1)-PAG in 3D WSNs.

6.2 Performance Metrics

We investigate four performance metrics, including energy consumption, network lifetime, packet delivery ratio, and delivery delay, to evaluate our scheme.

- The energy consumption is defined as the total energy consumed by all sensor nodes which have participated in data delivery. This metric indicates how much energy is consumed by all the sensor nodes for communications.
- The network lifetime is defined as a period from simulation beginning to time instant that nodes deplete their 20% or more energy in the network.

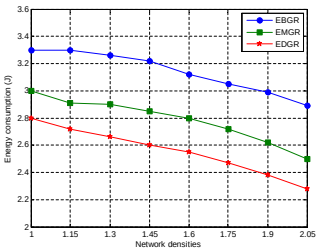

(a) energy consumption

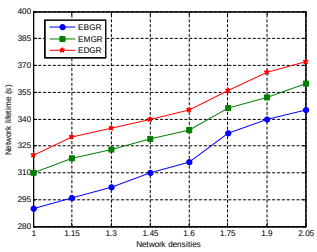

(b) network lifetime

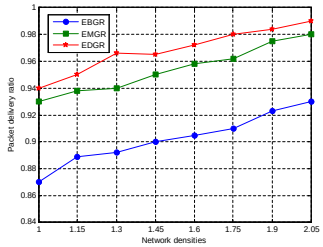

(c) packet delivery ratio

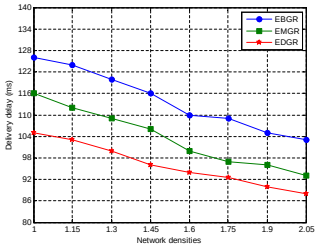

(d) delivery delay

Fig. 7: Performance of three approaches with varied network densities.

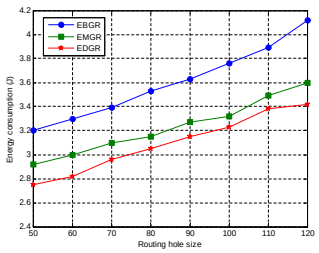

(a) energy consumption

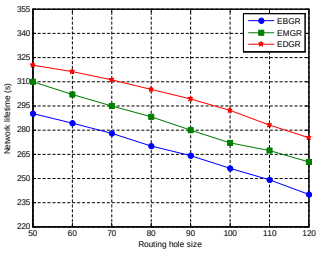

(b) network lifetime

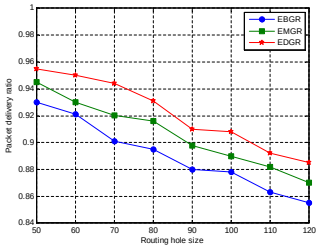

(c) packet delivery ratio

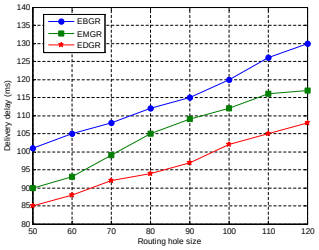

(d) delivery delay

Fig. 8: Performance of three approaches with varied hole sizes.

This metric indicates the degree of load balance among nodes involved in communications.

- The packet delivery ratio is defined as the ratio between the number of successfully delivered data packets and the number of data packets generated by the source node. This metric reflects the data delivery efficiency.
- The delivery delay is defined as the time delay from the generation of the packet to its delivery to the destination. This metric indicates how quick the data packets are received by destination after being sent from the source node.

6.3 Performance of EDGR with Varied Network Densities

In this subsection, one routing hole with the average diameter of $60m$ is set in the network. We fix the number of communication sessions as 4, and vary the network density from 1.0 (i.e., $\rho_1 = 400 * \frac{3.14*40^2}{1000^2-3.14*30^2} - 1$) neighbors/node to 2.1 (i.e, $\rho_2 = 600 * \frac{3.14*40^2}{1000^2-3.14*30^2} - 1$) neighbors/node to evaluate the performance of the proposed approach.

Fig. 7(a) displays the total energy consumption of EDGR, EBGR and EMGR with different network densities. It is clear to see that there is considerable energy-reduction as the network density increases for three protocols because the density helps them find out more energy-efficient paths. Compared to EBGR and EMGR, EDGR achieves a similar energy-reduction while 9.3% and 3.7% longer average network lifetime, respectively, illustrated in Fig. 7(b), since it can search more energy-efficient paths located in two sides of the routing holes for further load balance in data delivery.

Fig. 7(c) demonstrates the packet delivery ratio with different network densities. The results indicate that all three protocols have higher packet delivery ratio under a higher network density. This is because all of them can find more efficient paths for data delivery. Compared to EBGR and EMGR, our proposed approach has up to 10.6% and 3.1% higher packet delivery ratio, respectively, due to less data collisions occurring in the hole boundary. Specifically, EDGR exploits two paths, passing through two sides of routing holes rather than one side to forward data, thus improving packet delivery ratio.

Fig. 7(d) indicates the delivery delay of EDGR, EBGR and EMGR with different network densities. It is seen that all three protocols achieve a smaller delivery delay as the network density increases since the density helps three protocols find out more efficient paths to deliver data. The results show that the delivery delay of our protocol is lower than EBGR and EMGR as the network density increases. The main reason is that we introduce anchor list passing through two sides of the routing holes to redirect data delivery, meaning that the paths are spatially dispersed to avoid unwanted data collisions and become shorter.

6.4 Performance of EDGR with Varied Hole Sizes

In this subsection, we fix the number of communication sessions as 4, and manually set a routing hole with various sizes (diameters) from $50m$ (i.e, $d_1 = 50$) to $120m$ (i.e, $d_2 = 120$) in the center of the network to evaluate the effect of the hole size.

Fig. 8(a) demonstrates the average energy consumption of nodes when the hole size varies from $50m$ to $120m$. It is observed that there is a great energy-increase for three protocols as the hole size increases because the

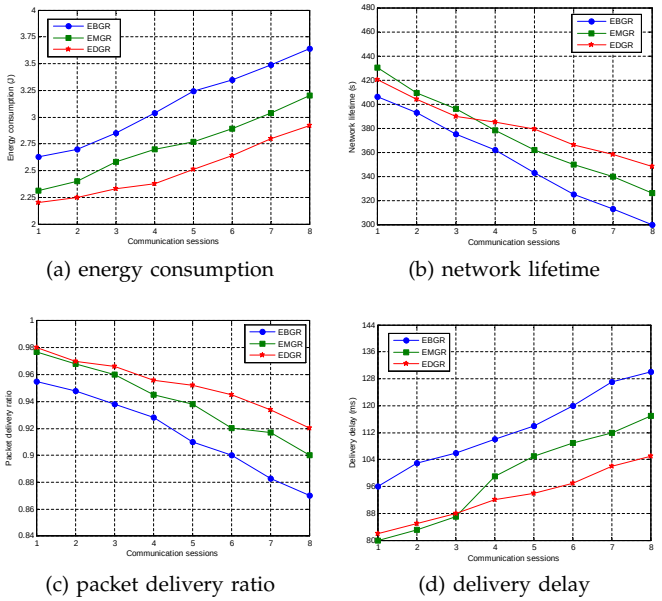

(a) energy consumption (b) network lifetime

(c) packet delivery ratio (d) delivery delay

Fig. 9: Performance of three approaches with varied communication sessions.

routing hole makes the paths for data delivery longer and more curvy. Compared to EBGR, both EDGR and EMGR achieve a similar energy-reduction while 12.8% and 6.5% longer average network lifetime, respectively, elaborated in Fig. 8(b), since the data is redirected to destination along multiple paths once encountering a routing hole. The results indicate that EDGR outperforms EMGR in term of network lifetime, since it exploits two separated paths, passing through two sides of the routing holes, to shift the routing for further load balance in data delivery.

Fig. 8(c) displays the packet delivery ratio of EDGR, EBGR and EMGR with different hole sizes. It shows that, the packet delivery ratio of three protocols distinctly decreases due to data collisions occurring in the hole boundary. Compared to EBGR, both EDGR and EMGR are redirected to anchor nodes once a routing hole exists, thus helping data collisions decrease to achieve the better packet delivery ratio. The results indicate that the packet delivery ratio of EDGR fluctuates comparatively less than EMGR since it exploits two separated paths, passing through two sides of the routing holes, to deliver data with less data collisions.

Fig. 8(d) shows the delivery delay with varied hole sizes. The results show that the delivery delay of our approach is lower than EBGR and EMGR as the hole size increases. The main reasons are summarized as follows: referring to date collisions, routing length and the number of paths. First, EDGR introduces anchor nodes to guide data delivery once a routing hole exists, thus shortening the paths and finding multipath routing for data delivery compared to EBGR. Second, EDGR exploits two separated paths to forward data, avoiding unwanted data collisions.

TABLE 2: Data Collisions with Different Communication Sessions

Communication Sessions	Data Collisions		
	EBGR	EMGR	EDGR
1	-	-	-
2	1.0	0.7	0.5
3	2.8	1.9	1.6
4	6.2	4.0	3.5
5	9.4	6.2	5.1
6	15.2	10.8	7.6
7	19.6	12.7	8.2
8	23.3	14.3	11.6

6.5 Performance of EDGR with Varied Communication Sessions

In this subsection, two routing holes with the initial size of $60m$ are set in the center of the network, and the number of communication sessions varies from 1 (i.e, $N_1 = 1$) to 8 (i.e, $N_2 = 8$).

Fig. 9(a) demonstrates the total energy consumption of EBGR, EMGR, and EDGR with different communication sessions. It is easy to see that the energy consumption of EBGR is quite higher than that of EMGR. This phenomenon can be explained as follows: in the scenarios with different communication sessions, EMGR prevents data from being forwarded along the boundary of routing holes, thereby shortening the routing length and hence conserving the energy. Compared to EMGR, in our scheme the data packets are routed to destination along two different paths which respectively pass through two sides of the routing holes with less data collisions. In this way, less energy is consumed for retransmissions. So, the energy consumption of our approach increases slightly than EBGR and EMGR with different communication sessions.

Fig. 9(b) indicates the network lifetime of EBGR, EMGR, and EDGR with different communication sessions. The results show that both EDGR and EMGR significantly extend the network lifetime compared to EBGR. This is because both of them route data packets to each destination along energy-efficient multi-path rather than one path for EBGR, thus balancing energy conservation among nodes in the network. Compared to EMGR, EDGR routes data packets to each destination along two different paths not more paths but with more residual energy, and avoids unwanted collisions occurring in the paths since such two paths locate in two different sides of the routing holes, thereby consuming a little more energy in each node on the paths. As a consequence the network lifetime of EDGR changes slightly than EMGR as the number of communication sessions increases.

Fig. 9(c) illustrates the packet delivery ratio with different communication sessions. With the number of communication sessions increasing, multiple communication sessions may simultaneously bypass a routing hole, resulting in high packet drop ratio for EBGR, EMGR and our scheme. This is mainly due to the data collisions occurring in data delivery on the boundary of the

routing holes. In order to facilitate the understanding, we list the existing data collisions of EBGR, EMGE and EDGR in TABLE 2, represented with the total number of communication session pairs which pass through the same paths, crossing links, and adjacent links or paths on the boundary of the routing holes. In our scheme, the data packets are redirected to the anchor nodes located in two sides of the routing holes. Because the anchor nodes are different with various source-destination pairs and the paths are far for fixed source node and destination, the data collisions seldom occur. So, the packet delivery ratio of our scheme does not significantly decrease when the number of communication sessions increases.

Fig. 9(d) displays the delivery delay with different communication sessions. The results indicate that our scheme achieves the lowest delivery delay compared to EBGR and EMGR when the number of communication sessions exceeds 3. There are mainly two reasons for the performance gap in our scheme with EBGR and EMGR. First, we introduce two node-disjoint anchor lists to guide data delivery, thus significantly shortening the routing path. Second, we route data packets to destination along two different spaced paths located in two sides of the routing holes. Such a case can lower data collisions occurring in data delivery as the number of communication sessions increases, thus decreasing the number of retransmissions and reducing the queue and transmission delay.

6.6 Performance of EDGR-2 with Varied Communication Sessions

In this subsection, the network size is set to be $1000m \times 1000m \times 1000m$. One routing hole with the initial size of $60m$ is set in the center of the network. The number of communication sessions varies from 1 (i.e, $N_1 = 1$) to 8 (i.e, $N_2 = 8$), and the factor β for PAG-CFace(1)-PAG to increase transmission radius varies in the range $[1.2, 2.2]$ following [25].

Fig. 10(a) depicts the total energy consumption of EDGR-2 and PAG-CFace(1)-PAG in 3D WSNs. It shows that, the energy consumption of EDGR-2 is smaller than that of PAG-CFace(1)-PAG. For example, when the number of communication sessions is 3, the energy consumption used by EDGR-2 is 10.5% less than that of PAG-CFace(1)-PAG. Compared to PAG-CFace(1)-PAG, the data packets in our scheme are routed to destinations along two different paths in an energy-efficient manner, by selecting the forwarders from energy-aware relay region. Once encountering a routing hole, it projects the nodes into a 2D plane and EDGR is employed to continue data delivery, while PAG-CFace(1)-PAG only employs CFace(1) to deal with this case. So, our scheme consumes less energy with different number of communication sessions.

Fig. 10(b) illustrates the network lifetime of EDGR-2 and PAG-CFace(1)-PAG in 3D WSNs with different communication sessions. It is observed that EDGR-2 achieves

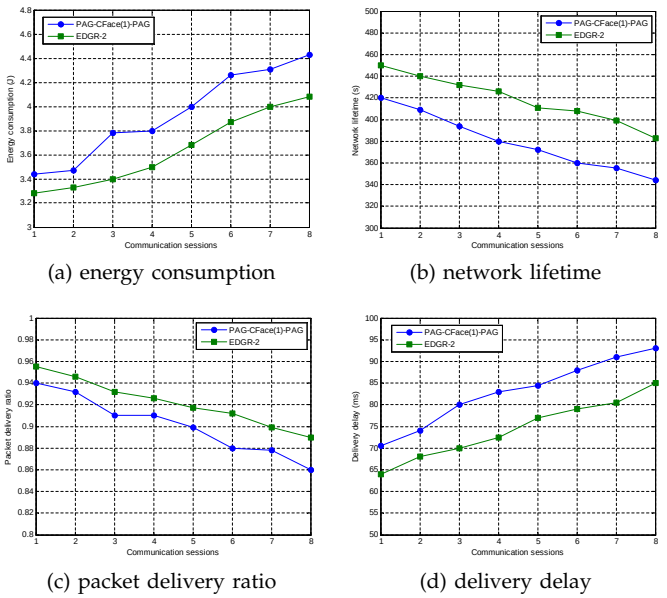

(a) energy consumption (b) network lifetime

(c) packet delivery ratio (d) delivery delay

Fig. 10: Performance of two 3D approaches with varied communication sessions.

the longer network lifetime compared to PAG-CFace(1)-PAG. This phenomenon can be explained as follows. EDGR-2 projects 3D nodes into xy, yz, xz planes once encountering a routing hole in 3D WSNs, then performs EDGR routing in the planes. In this way, each data flow will be routed to destination along two energy-aware paths not an energy-agnostic path for PAG-CFace(1)-PAG, and therefore, more nodes with much more residual energy are involved in data delivery, thus balancing the network load in the whole network. Therefore, EDGR-2 can significantly extend network lifetime as the numbers of communication sessions increases.

Fig. 10(c) indicates the packet delivery ratio of EDGR-2 and PAG-CFace(1)-PAG in 3D WSNs. The results demonstrate that our scheme achieves the better packet delivery ratio compared to PAG-CFace(1)-PAG. The obvious reason is that EDGR-2 projects the nodes into xy, yz, xz planes to find possible paths for data delivery once encountering a routing hole in 3D WSNs, while PAG-CFace(1)-PAG in one plane only, e.g., xy plane, tries to do it, thus EDGR-2 distinctly guarantees data delivery.

Fig. 10(d) demonstrates the delivery delay of EDGR-2 and PAG-CFace(1)-PAG in 3D WSNs with different numbers of communication sessions. It is shown that EDGR-2 achieves the lower delivery delay compared to PAG-CFace(1)-PAG. This phenomenon can be explained as follows. Once encountering a routing hole in 3D WSNs, EDGR-2 employs two possible paths rather than a path for PAG-CFace(1)-PAG to continue data delivery in a 2D plane, thus achieving load balance and decreasing delivery delay.

7 Related Work

In the past decade, a variety of geographic routing protocols have been proposed, such as [3], [4], [6], [7],

[8], [10], [11] [12], [13], [16], to address the routing hole issues occurring in WSNs. A comprehensive survey of geographic routing protocols regarding how to bypass the routing holes can be found in [2], [5]. Commonly, these proposed protocols utilize greedy mode to route data packets as far as possible and switch to bypass mode for route recovery once encountering a routing hole.

Currently, most geographic routing protocols, such as GFG and GPSR, tend to route data along the boundary of the routing holes for route recovery by employing face routing scheme [4], [6], [12]. Once the bypass mode is involved in the routing, these combinatorial protocols cannot guarantee that all packets are delivered in an energy-efficient manner since they tend to generate long path and hence consume additional energy during routing packets. Beyond face routing, there are also other approaches [5], [7], [11], [16] used to recover the route. The basic idea of these approaches is to localize routing holes before data delivery and then to derive a detour path with anchor nodes, such that the data is routed to desired destination in an energy-aware manner. However, all of the above-mentioned approaches only walk along one side of the routing holes to recover the route, thus making the load converged on the boundary of the routing holes.

Notice that sensor nodes are energy constrained and battery recharging is often infeasible, a large number of energy-aware geographic routing protocols [18], [19], [20], [21], [22], [23], [24], [25], [26], [27], [28] have, therefore, been proposed for WSNs. With the knowledge of neighbor information, these approaches employ energy-aware criteria rather than traditional routing metrics such as hop count or delay to make routing decisions. Classical energy-aware criteria include power, cost, power-cost, power-to-advance/progress ratio and cost-to-advance/progress ratio [18], [21], [25]. A first set of energy-aware approaches stems from the work of Stojmenovic et al. [19]. Most further studies mainly focus on energy-efficient path establishment [18], energy-efficient multicast data delivery [20], energy consumption balance [22], communication overhead reduction [23], [24], better route recovery from routing holes [27], [28], or the combination of locations and other energy-aware factors in routing [2], [34], [38]. In addition, the work in [25], [34] has proposed 3D geographic routing approaches for energy conservation, based on the idea of replacing the constant transmission power of the node with an adjusted transmission power [25] or optimizing the 3D paths in different curve surfaces [34].

So far, only a limited number of energy-aware geographic routing protocols [11], [26], [27], [28] have taken into consideration the load balance for route recovery from routing holes. Specifically, Wu et al. [26] proposed several power-aware techniques that attempt to balance the traffic among the nodes to extend the network lifetime. In [26], each forwarder first establishes a subdestination among its one-hop neighbors, and then routes the data to it through an intermediary node or alters the subdestination if this will preserve power. Similar to [26], Zhao et al. [27] suggested balancing the traffic to conserve energy, by randomly shifting the location of each anchor node. The work in [28] proposed an energy-aware multipath geographic routing to balance load, by exploiting a dynamic anchor list passing through one side of the routing holes to shift routing path. However, it cannot provide simultaneous transmissions for a fixed source-destination pair along multiple paths due to the potential data collisions among them. What is more, all these approaches [26], [27], [28] are efficient only in 2D WSNs while not being extended into 3D WSNs.

8 Conclusions

In this paper, we propose EDGR, a novel energy-aware dual-path geographic routing protocol, to better recover the route from routing holes for WSNs. In EDGR, two node-disjoint anchor lists are provided to shift routing path for load balance, and the location information, residual energy and energy characteristics of nodes are employed to make routing decisions, thereby enabling an energy-aware dual-path routing strategy. EDGR is practical, feasible and scalable. Simulation results show that EDGR exhibits lower energy consumption, fairly longer network lifetime, moderately better packet delivery ratio, and comparatively smaller delivery delay than other geographic routing protocols in WSNs over a variety of communication scenarios passing through routing holes.

Acknowledgments

This work has been partially supported by the National Natural Science Foundation of China (No. 61402343, No. 61672318, No. U1504614, No. 61631013, and No. 61303241), the National Key Research and Development Program (No. 2016YFB1000102), the Natural Science Foundation of Suzhou/Jiangsu Province (No. BK20160385), the EU FP7 QUICK Project (No. PIRSES-GA-2013-612652), and the projects of Tsinghua National Laboratory for Information Science and Technology (TNList).

References

[1] L. Cheng, J. Niu, J. Cao, S. Das, and Y. Gu, "QoS Aware Geographic Opportunistic Routing in Wireless Sensor Networks," *IEEE Trans. Parallel Distrib. Syst.*, vol. 25, no. 7, pp. 1864-1875, Jul. 2014.

[2] C. Fraser, C. Kevin, S. Jose, and M. Sandra, "A Survey of Geographical Routing in Wireless Ad-Hoc Networks," *IEEE Commun. Surv. Tutor.*, vol. 15. no. 2, pp. 621-653, 2013.

[3] S. S. Lan and C. Qian, "Geographic Routing in *d*-Dimensional Spaces with Guaranteed Delivery and Low Stretch," *IEEE/ ACM Trans. Netw.*, vol. 21, no. 2, pp. 663-677, 2013.

[4] B. Karp and H. Kung, "GPSR: Greedy Perimeter Stateless Routing for Wireless Networks," *Proc. ACM MobiCom 2000*, Boston, Massachusetts, USA, pp. 243-254, 2000.

[5] D. Chen and P.K. Varshney, "A Survey of Void Handling Techniques for Geographic Routing in Wireless Networks," *IEEE Commun. Surv. Tutor.*, vol. 9, no. 1, pp. 50-67, 2007.

[6] P. Bose, P. Morin, I. Stojmenovic, and J. Urrutia, "Routing with Guaranteed Delivery in Ad Hoc Wireless Networks," *ACM/Kluwer Wireless Netw.*, vol. 7, no. 6, pp. 609-616, 2001.
[7] W. Liu and K. Feng, "Greedy Routing with Anti-void Traversal for Wireless Sensor Networks," *IEEE Trans. Mob. Comput.*, vol. 8, no. 7, pp. 910-922, 2009.
[8] Q. Chen, S. S. Kanhere, and M. Hassan, "Adaptive Position Update for Geographic Routing in Mobile Ad Hoc Networks," *IEEE Trans. Mob. Comput.*, vol. 12, no. 3, pp. 489-501, Mar. 2013.
[9] H. Frey and I. Stojmenovic, "On Delivery Guarantees of Face and Combined Greedy Face Routing in Ad Hoc and Sensor Networks," *Proc. ACM MobiCom 2006*, CA, USA, pp. 390-401, 2006.
[10] Q. Fang, J. Gao, and L. J. Guibas, "Located and Bypassing Routing Holes in Sensor Networks," *Proc. IEEE INFOCOM 2004*, Hong Kong, China, pp. 2458-2468, Mar. 2004.
[11] C. Petrioli, M. Nati, P. Casari, M. Zorzi, and S. Basagni, "ALBA-R: Load-balancing Geographic Routing Around Connectivity Holes in Wireless Sensor Networks," *IEEE Trans. Parallel Distrib. Syst.*, vol. 25, no. 3, pp. 529-539, Mar. 2014.
[12] X. Xiang, X. Wang, and Z. Zhou, "Self-Adaptive On-Demand Geographic Routing for Mobile Ad Hoc Networks," *IEEE Trans. Mob. Comput.*, vol. 11, no. 9, pp. 1572-1586, Sept. 2012.
[13] X. Li, J. Yang, A. Nayak, and I. Stojmenovic, "Localized Geographic Routing to a Mobile Sink with Guaranteed Delivery in Sensor Networks," *IEEE J. Selected Areas in Comm.*, vol. 30, no. 9, pp. 1719-1729, Oct. 2012.
[14] S. Ruhrup and I. Stojmenovic, "Optimizing Communication Overhead while Reducing Path Length in Beaconless Georouting with Guaranteed Delivery for Wireless Sensor Networks," *IEEE Trans. Comput.*, vol. 62, no. 12, pp. 2240-2253, Dec. 2013.
[15] X. Wang, J. Wang, K. Lu, and Y. Xu, "GKAR: A Novel Geographic K-anycast Routing for Wireless Sensor Networks," *IEEE Trans. Parallel Distrib. Syst.*, vol. 24, no. 5, pp. 916-925, 2013.
[16] A. Mostefaoui, M. Melkemi, and A. Boukerche, "Localized Routing Approach to Bypass Holes in Wireless Sensor Networks", *IEEE Trans. Comput.*, no. 63, no. 12, pp. 3053-3065, Dec. 2014.
[17] G. Tan and A. M. Kermarrec, "Greedy Geographic Routing in Large-Scale Sensor Networks: A Minimum Network Decomposition Approach," *IEEE/ACM Trans. Netw.*, vol. 20, no. 3, pp. 864-877, Jun. 2012.
[18] J. Sanchez and P. Ruiz, "Locally Optimal Source Routing for Energy-efficient Geographic Routing," *ACM/Kluwer Wireless Netw.*, vol. 15, no. 4, pp. 513-523, May 2009.
[19] I. Stojmenovic and X. Lin, "Power-aware Localized Routing in Wireless Networks," *IEEE Trans. Parallel Distrib. Syst.*, vol. 12, no. 11, pp. 1122-1133, 2001.
[20] J. Sanchez, P. Ruiz, and I. Stojmenovic, "Energy-efficient Geographic Multicast Routing for Sensor and Actuator Networks," *Wilel. Commun. Mob. Comput.*, vol. 30, no. 13, pp. 2519-2531, 2007.
[21] J. Kuruvila, A. Nayak, and I. Stojmenovic, "Progress and Location Based Localized Power Aware Routing for Ad Hoc and Sensor Wireless Networks," *Hhindawi Int. J. Distrib. Sen. Netw.*, vol. 2, no. 2, pp. 147-159, 2006.
[22] Y. Yan, G. Ramesh, and E. Deborah, "Geographic and Energy Aware Routing: A Recursive Data Dissemination Algorithm for Wireless Sensor Networks," UCLA/CSD-TR-01-0023, 2001.
[23] H. Zhang and H. Shen, "EEGR: Energy-efficient Geographic Routing in Wireless Sensor Networks," *Proc. IEEE ICPP 2007*, Xian, China, pp. 67-74, Sep. 2007.
[24] H. Zhang and H. Shen, "Energy-efficient Beaconless Geographic Routing in Wireless Sensor Networks," *IEEE Trans. Parallel Distrib. Syst.*, vol. 21, no. 6, pp. 881-896, Jun. 2010.
[25] A. E. bdallah, T. Fevens, and J. Opatrny, "Power-aware Semi-beaconless 3D Geographic Routing Algorithms Using Adjustable Transmission Ranges for Wireless Ad Hoc and Sensor Networks," *Elsevier Ad Hoc Netw.*, vol. 8, no. 1, pp. 15-29, Jan. 2010.
[26] S. Wu and K. S. Candan, "Power-aware Single and Multipath Geographic Routing in Sensor Networks," *Elsevier Ad Hoc Netw.*, vol. 5, no. 7, pp. 974-997, Jun. 2006.
[27] G. Zhao, X. Liu, and M. T. Sun, "Energy-efficient Geographic Routing with Virtual Anchors Based on Projection Distance," *Elsevier Comp. Commu.*, vol. 31, no. 10, pp. 2195-2204, Jun. 2008.
[28] H. Huang, G. Hu, and F. Yu, "Energy-aware Multipath Geographic Routing for Detouring Mode in Wireless Sensor Networks," *Wiley Eur. Trans. Telecomm.*, vol. 22, no. 7, pp. 375-387, 2011.
[29] W. Yu, Ch. Yi, M. Huang, and F. Li, "Three-dimensional Greedy Routing in Large-scale Random Wireless Sensor Networks," *Elsevier Ad Hoc Netw.*, vol. 11, no. 4, pp. 1331-1344, 2013.
[30] A. M. tahan and M. K. Watfa, "A Position-based Routing Algorithm in 3D Sensor Networks," *Wiley. Commun. Mob. Comput.*, vol. 12, no. 1, pp. 33-52, Jan. 2012.
[31] J. Bruck, J. Gao, and A. Jiang, "Localization and Routing in Sensor Networks by Local Angle Information," *ACM Trans. Sen. Netw.*, vol. 5, no. 1, pp. 1-31, Feb. 2009.
[32] R. Coutinho, A. Boukerche, L. Menezes Vieira, and A. Loureiro, "Geographic and Opportunistic Routing for Underwater Sensor Networks," *IEEE Trans. Comput.*, vol. 65, no. 2, pp. 548-561, Mar. 2016.
[33] R. Flury and R. Wattenhofer, "Randomized 3D Geographic Routing," *Proc. IEEE INFOCOM 2008*, Phoenix, AZ, pp. 834-842, 2008.
[34] H. Huang, H. Yin, Y. Luo, X. Zhang, G. Min and Q. Fan, "Three-dimensional Geographic Routing in Wireless Mobile Ad Hoc and Sensor Networks," *IEEE Network Mag.*, vol. 30, no. 2, pp. 82-90, Mar. 2016.
[35] A. E. Abdallah, T. Fevens, and J. Opatrny, "Randomized 3-d Position-based Routing Algorithm for Ad Hoc Networks," *Proc. IEEE Mobiquitous 2006*, CA, USA, pp. 1-8, Jul. 2006.
[36] Http://mathworld.wolfram.com/circle-circleintersection.html.
[37] J. Wang, R. K. Ghosh, and S. K. Das, "A Survey on Sensor Localization," *Springer J. Cont. Theo. App.*, vol. 8, no. 1, pp. 2-11, Feb. 2010.
[38] D. Torrieri, S. Talarico, and M. Valenti, "Performance Comparisons of Geographic Routing Protocols in Mobile Ad Hoc Networks," *IEEE Trans. Comm.*, vol. 63, no. 11, pp. 4276-4286, 2015.

Haojun Huang is an assistant professor in Communication Engineering within the College of Electronic Information Engineering at Wuhan University. He received his BS degree in School of Computer Science and Technology from Wuhan University of Technology in 2005, and his PhD degree in School of Communication and Information Engineering from the University of Electronic Science and Technology of China in 2012. He worked as a postdoctor in the Research Institute of Information Technology at Tsinghua University from 2012 to 2015. His current research interests include wireless communication, Ad Hoc networks, Big Data, and Software-Defined Networking.

Hao Yin is a Professor in the Research Institute of Information Technology (RIIT) at Tsinghua University. He received the BS, ME, and PhD degrees from Huazhong University of Science and Technology, Wuhan, China, in 1996, 1999, and 2002,respectively, all in electrical engineering. He was elected as the New Century Excellent Talent of the Chinese Ministry of Education in 2009, and won the Chinese National Science Foundation for Excellent Young Scholars in 2012. His research interests span broad aspects of Multimedia Communication and Computer Networks.

Geyong Min is a Professor of High Performance Computing and Networking in the Department of Mathematics and Computer Science within the College of Engineering, Mathematics and Physical Sciences at the University of Exeter, United Kingdom. He received the PhD degree in Computing Science from the University of Glasgow, United Kingdom, in 2003, and the BS degree in Computer Science from Huazhong University of Science and Technology, China, in 1995. His research interests include Future Internet, Computer Networks, Wireless Communications, Multimedia Systems, Information Security, High Performance Computing, Ubiquitous Computing, Modelling and Performance Engineering.

Junbao Zhang worked as an assistant professor of computer science in Zhongyuan University of Technology from 2012 to the present. He received his PhD degree from the Department of Computer Science at the University of Electronic Science and Technology of China, China, in 2012. His research areas include delay tolerant networks, sensor networks and vehicular Ad Hoc networks.

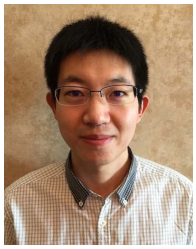

Yulei Wu is a Lecturer in Computer Science at the University of Exeter. He received his PhD degree in Computing and Mathematics and BS (First Class Hons) degree in Computer Science from the University of Bradford, UK, in 2010 and 2006, respectively. His main research focuses on Future Internet Architecture and Technologies, Smart Network Management, Cloud Computing, Big Data for Networking, and Analytical Modelling and Performance Optimisation.

His recent research has been supported by Industrial KTP, Huawei Technologies, London Mathematical Society, National Natural Science Foundation of China, and University's Innovation Platform. He has published over 50 research papers in prestigious international journals and at reputable international conferences.

Xu Zhang is an Assistant Researcher in the School of Electronic Science and Engineering, Nanjing University, Nanjing, Jiangsu, China. He received the BS degree in communication engineering from the Beijing University of Posts and Telecommunications, Beijing, China, in 2012 and the PhD degree from the Department of Computer Science and Technology, Tsinghua University, Beijing, China, in 2017. He was a visiting student in the Department of Electrical and Computer Engineering, University of Florida, Florida, from 2015 to 2016. His research interests include content delivery networks, network measurement, and cloud computing.